

A CONSISTENT COUPLING OF NODAL EXPANSION METHOD, ANALYTIC NODAL METHOD, AND FINITE DIFFERENCE METHOD FOR 3-DIMENSIONAL REACTOR CORE ANALYSIS

DeokJung Lee, YongHee Kim, and YongBae Kim
Korea Electric Power Research Institute
103-16, Yusung-Ku, Munji-Dong, Taejon, Korea, 305-380
djlee@kepri.re.kr ; kyhee@kepri.re.kr ; ybkim@kepri.re.kr

ABSTRACT

A high order and low order hybrid method has been proposed for the efficient and accurate 3-dimensional LWR core analysis. This method uses nodal expansion method (NEM) or analytic nodal method (ANM) for coarse-mesh z-directional coupling and fine-mesh finite difference method (FDM) in x-, y-direction. NEM, ANM, and FDM are consistently coupled using the node interface currents and the transverse leakage. The advantage of the new hybrid method is that no homogenization/dehomogenization is required and fine-mesh FDM comparable results can be achievable within reasonable time. When control rods are inserted into a core consisting of heterogeneous assemblies, the flux and transverse leakage change dramatically around the tip of the control rod. Consequently, the conventional NEM and transverse leakage approximations do not work well. These problems were overcome successfully by applying partially ANM for the flux calculation and obtaining the transverse leakage shape from a small local problem which is defined in the neighborhood of the tip of control rod. The benchmark calculations demonstrate that the new method is numerically stable and accurate enough to be applied to 3-dimensional reactor core analyses, and also much faster than the conventional fine-mesh FDM.

1. INTRODUCTION

Currently, nodal methods such as NEM¹ and ANM² are exclusively favored in the LWR core analysis with the aid of the assembly homogenization³ techniques due to the fact that the calculation speed of nodal method is much faster and the accuracy of the results is not so bad compared with fine-mesh FDM⁴ results. But nodal method itself does not give any local information such as pin-wise powers required in real core design, therefore the dehomogenization procedures are inevitable⁵. Meanwhile, even though the fine-mesh FDM can give the local power distributions directly, it needs so long

calculation time that it is inappropriate for the practical core design calculation.

The objective of the present work is to develop an efficient nodal and fine-mesh FDM hybrid algorithm which can provide accuracy comparable to that of the fine-mesh FDM for a 3-dimensional LWR core analyses subjected to the pin cell-wise cross sections, i.e., without the assembly homogenization. The present work is based on the fact that the material properties of a LWR core are fairly homogeneous in the axial direction, compared against the radial directions. This fact implies that a coarse mesh nodal method could be applied for the z-directional calculation without compromising the accuracy. Unfortunately, it does not hold around the tip of the control rod where the conventional nodal methods have large errors due to the lack of ability to approximate the rapidly-varying transverse leakage. To resolve the problem, a global/local iteration is introduced, where a small local problem is analyzed in a spectral geometry and the local solution is used in synthesizing the shape of the transverse leakage.

2. METHODOGY

The following is the 3-dimensional neutron balance equation to be solved.

$$\nabla \cdot \mathbf{J}_g(r) + \Sigma_{rg}(r) \mathbf{f}_g(r) = \sum \left(\frac{\mathbf{c}_g}{k_{eff}} \mathbf{r} \Sigma_{fg}(r) + \Sigma_{sgg} \right) \mathbf{f}_g(r), \quad (1)$$

where all notations are standard.

The nodal and FDM hybrid method is consisted of the inner iteration and the outer iteration like as the conventional schemes. But the unique point of this new method is that the inner iteration is consisted of successive 2-dimensional FDM calculations for each plane and inter-plane partial current couplings. And it is also a noticeable point that the z-directional flux shape in the source term expressed by the expansion coefficients of NEM flux should be fixed during the inner iteration of the same outer iteration step for the stable convergence.

In the new method, The coupling between the adjacent planes are established by using the partial currents at each interface. Although one can also couple the planes with the net interface currents, the performance is lower than the partial current coupling in convergence point of view. Therefore, the 2-dimensional FDM formulation uses directly the incoming currents from the adjacent nodes and they are directly available from the z-directional nodal solutions.

Eq. (1) is approximated by FDM in each radial plane and they can be written as below for node m.

$$b_g^W \mathbf{f}_g^W + b_g^E \mathbf{f}_g^E + b_g^S \mathbf{f}_g^S + b_g^N \mathbf{f}_g^N + b_g^m \mathbf{f}_g^m = s_g^m, \quad (2)$$

where $b_g^n = -\frac{2}{h_u^m} \frac{\mathbf{b}_{gu}^m \mathbf{b}_{gu}^n}{\mathbf{b}_{gu}^m + \mathbf{b}_{gu}^n}$, $b_g^m = -\sum_{n=W,E,S,N} b_g^n + \Sigma_{rg}^m + \frac{2C_{1gz}^m}{h_z^m}$, $\mathbf{b}_{gu}^m = \frac{D_g^m}{h_u^m}$, $C_{1g}^m = \frac{6\mathbf{b}_g^m}{1+12\mathbf{b}_g^m}$,

$$s_g^m = \left(\frac{\mathbf{c}_g}{k_{eff}} \mathbf{n} \Sigma_{fg'}^m + \Sigma_{sgg'}^m \right) \mathbf{f}_{g'}^m + \frac{2C_{1gz}^m}{h_z^m} (2(j_{gzL}^{+m} + j_{gzR}^{-m}) - a_{4gz}^m),$$

$j_{gzs}^{\pm m}$ = partial current at surface,

a_{4gz}^m = flux expansion 4th-order coefficient for of z-directional flux.

This equation is same as the standard FDM formulation except that the current terms at the inter-plane interface are expressed by the incoming currents using conventional NEM formulation.

On the other hand, the NEM approximation for z-direction can be represented in the following equation.

$$\left(\Sigma_{rg}^m + \frac{2C_{1g}^m}{h_z^m} \right) \mathbf{f}_g^m = \left(\frac{\mathbf{c}_g}{k_{eff}} \mathbf{n} \Sigma_{fg'}^m + \Sigma_{sgg'}^m \right) \mathbf{f}_{g'}^m + \frac{2C_{1g}^m}{h_z^m} (2(j_{gzL}^{+m} + j_{gzR}^{-m}) - a_{4g}^m) - L_{gz}^m, \quad (3)$$

where $L_{gz}^m = \sum_{n=W,E,S,N} [p_g^n \mathbf{f}_g^n] + p_g^m \mathbf{f}_g^m$,

$$p_g^m = -p_g^W - p_g^E - p_g^S - p_g^N,$$

$$p_g^n = -\frac{1}{h_u^m} \frac{2\mathbf{b}_{gu}^m \mathbf{b}_{gu}^n}{(\mathbf{b}_{gu}^m + \mathbf{b}_{gu}^n)}.$$

The transverse leakage in the above equation is obtained by a linear approximation of flux in radial direction using node average flux from radial FDM solutions. To find the solutions of Eq. (1) in the whole reactor core, Eqs. (2) and (3) are repeatedly solved updating the transverse leakages.

In principle, any nodal method can be used for the z-directional coarse-mesh calculation. In this work, ANM also was used partially in the region where 4th-order NEM does not show a sufficient performance. For the z-directional inter-plane partial current, the coefficients of ANM basis should be determined using only incoming currents from upper and lower planes, which is different from conventional ANM net current coupling.

The z-directional transverse leakage was approximated as a quadratic form as in the conventional nodal methods. But as shown in the following numerical test section, the transverse leakage shape could be deformed so much that the conventional determination method of the quadratic expansion coefficients is not enough to represent the dramatically-varying shape. This problem was overcome by adopting a global and local iteration strategy for the determination of the shape of transverse leakage. From the local solution, the accurate shape of z-directional transverse leakage is obtained and used for the determination of the transverse leakage expansion coefficients equivalent in the integral sense. The local problem is defined as a fixed boundary source problem. The boundary sources of local problems are updated at each global outer iteration using the global solution of the previous iteration step. For the overall performance, the local problem does not need to be fully converged because the information

used by global calculation is only the shape of transverse leakage which could be obtained with high accuracy with loose convergence.

3. NUMERICAL TESTS

To demonstrate the performance of the nodal and FDM hybrid algorithm, two benchmark problems were analyzed with a computer code developed using the new method. One is the IAEA3D PWR benchmark problem and the other is the modified EPRI-9R 3D problem. Even though both problems have partially inserted control rods, they are different in the aspect that the cross sections given in the former are assembly-wise homogenized cross sections and in the latter, cell-wise cross sections. The results of the two problems are compared with those of VENTURE code which uses the standard FDM.

The benchmark problems were solved by three solution strategies shown in Table I Method A is consisted of axial NEM calculation and radial FDM calculation with the conventional transverse leakage approximation. Method B uses the more exact shape of transverse leakage obtained from the local solutions for the meshes around the tip of control rods. The local problem is defined as a fixed boundary source problem consisted of 4 coarse meshes in z-direction with more local meshes and one assembly in radial direction around the tip of control rod for every rodded assembly. Additionally, method C adopted ANM partially instead of NEM around the tip of control rod because it is observed that 4th-order flux expansion of NEM cannot produce the dramatically varying flux shape around the tip of control rods.

3.1 IAED3D PWR BENCHMARK PROBLEM

The IAEA3D PWR benchmark problem was solved by method A. In this benchmark problem, the numerical tests were focused on the effects of the axial mesh size for a fixed plane mesh system ($\Delta x = \Delta y = 10$ cm). Basically, the two codes use the same method and the same mesh sizes for radial direction. Therefore, the results can be analyzed in the aspects of z-directional solution method and mesh system. Table II is the summary of the results. One can note that a nodal and FDM hybrid algorithm provides consistent solutions and the solution is very insensitive to the axial mesh size. The difference of eigenvalues between $\Delta z = 5$ cm and $\Delta z = 30$ cm is less than 2pcm. In other words, a very large axial mesh size, e.g., 20 cm, can be used with little compromise of the accuracy in the NEM/FDM hybrid method, if and only if the assemblies are homogenized a priori. Comparing the results of the new method and those of VENTURE, it is observed that the accuracy of the new algorithm with $\Delta z = 30$ cm is comparable to the VENTURE solution of $\Delta z = 1$ cm and the calculation speed is about 40 times faster.

3.2 MODIFIED EPRI-9R BENCHMARK PROBLEM

The EPRI-9R benchmark is a 2-dimensional problem with cell-wise heterogeneity but, in this study, it was modified to a 3-dimensional problem to verify the new method. The modified PERI-9R benchmark problem is shown in Figure 1. This problem is a quarter core with control rods inserted partially into the

mid-plane of the core. In the assembly structure, the black cells represent water cell or control rod cell. This problem was solved by 3 methods in Table I.

Table III is the summary of this benchmark calculation. Figures 2 through 5 show the axial shapes of the flux and transverse leakage of a rodded cell and Figures 6 through 9 show the axial shapes of the flux and transverse leakage of a adjacent fuel cell. In those figures, REF means reference solution generated by VENTURE using $\Delta z=1\text{cm}$ mesh size. It is observed that the flux and transverse leakage change dramatically around the tip of the control rods. The reason of this is that the material property changes abruptly at the tip of control rods (from the strong thermal neutron absorber to the efficient moderator). In general, highly deformed shapes, shown in Figure 2 through 9, cannot be observed in the conventional coarse-mesh nodal calculations using assembly-wise homogenized cross sections.

In method A, the difference of eigenvalues between $\Delta z=5\text{cm}$ and $\Delta z=20\text{cm}$ cases is 36pcm which is much bigger compared with the IAEA3D PWR benchmark results. Also, it is clear that, from Figures 2 through 9, the axial shapes of flux and transverse leakage of rodded cell and fuel cell have large error compared with the reference solutions. The main reason of this error is that the coefficients of transverse leakage expansion determined by the conventional method are not enough to simulate the steep transverse leakage in case of large axial mesh size. Namely, in this benchmark problem, method A cannot use coarse mesh in z-direction without loss of accuracy. But it is noticeable that the solution consistently approaches to the reference solution as the axial mesh size becomes smaller.

Method B based on the transverse leakage shapes from local solutions, shows better results. This method generates the transverse leakage shapes almost same as the reference and the error of eigenvalue decreased to 26pcm from 38pcm of method A. But as one can see in Figure 4, the thermal group flux shape of rodded cell has still a noticeable errors around the tip of control rod. This results show that even though the transverse leakage shape can be exactly evaluated, the 4th-order NEM cannot produce dramatically-varying flux shape sufficiently.

Therefore, we adopted ANM partially in the region around the tip of control rods where 4th-order NEM does not show high accuracy.

Method C gives more reasonable flux shape and so the error of eigenvalue decreased to 14pcm by 12pcm. The remaining error of 14pcm could be attributed partly to the effects of shape error around the axial reflectors as shown in Figure 4. and 5. and partly to the incomplete transverse leakage shape.

Figure 10. shows that all three methods predict the normalized radial power shape quite accurately in the sense of assembly average power and method C shows the best results out of them, as is expected. Figures 11. and 12. shows the radial power distribution of two adjoining planes separated by the control rod tip. In Figures 10. through 12., the results show the consistent behavior.

From the calculation time point of view, the difference of calculation time between method A and B could be thought of the time used for local calculation which is less than 5% of total calculation time. But due to the partial ANM calculation, the total calculation time increased by 17%, so in this work, NEM

is adopted mainly for the z-directional solution and ANM is used partially for the more accurate flux shape calculation

4. CONCLUSIONS

Two nodal methods NEM and ANM are consistently coupled with the FDM for efficient analysis of heterogeneous 3-dimensional reactor core which is composed of the heterogeneous assemblies. In the nodal and FDM hybrid method, each plane is solved by fine-mesh FDM and the consecutive planes are coupled via ANM or 4th-order NEM. For regions in which the flux and transverse leakage change dramatically, a global/local iteration strategy and ANM were introduced to improve the accuracy. The newly developed algorithm was compared with a standard fine-mesh FDM code (VENTURE) in terms of accuracy and calculation speed over the IAEA3D benchmark problem and a modified EPRI-9R 3D benchmark problem. Numerical results show that the nodal and FDM hybrid method is stable and provides consistent solutions. Also, about 20-times larger axial mesh size can be used in the new algorithm to obtain the accuracy comparable to the VENTURE solution. In addition, it is found that the new algorithm is several times faster than the VENTURE code. In the future works, we will improve the accuracy by introducing higher order approximations for the radial transverse leakage.

ACKNOWLEDGEMENTS

Authors would like to thank Dr. Eun Ki Lee (KEPRI) for his helpful comments about an efficient partial current coupling between planes.

REFERENCES

1. H. Finnemann and H. Raum, "Nodal Expansion Method for the Analysis of Space-Time Effects in LWRs," Proc. NEACRP Specialists' Meeting, Paris, November 26-28 (1979).
2. K. S. Smith, "An Analytical Nodal Method for Solving the Two-Group, Multidimensional, Static and Transient Neutron Diffusion Equations," Department of Nuclear Engineering Thesis, MIT, Cambridge, Massachusetts, March (1979).
3. K. S. Smith, A. F. Henry, and R. A. Loretz, "The Determination of Homogenized Diffusion Theory Parameters for Coarse Mesh Nodal Analysis," ANS Topical Meeting, Sun Valley, Idaho, September (1980).
4. Shoichiro Nakamura, *Computational Methods in Engineering and Science*, John Wiley & Sons Inc. (1977).

5. K. Koebke and Manfred R. Wagner, "The Determination Of The Pin Power Distribution In A Reactor Core On The Basis Of Nodal Coarse Mesh Calculations," Atomkernergie (ATKE) Bd. 30, pp. 136-142 (1977).

Table I. Three Schemes of Hybrid Method

METHOD	AXIAL	RADIAL	LOCAL PROBLEM
A	FULL NEM	FDM	NOT USED
B	FULL NEM	FDM	NEM+FDM
C	NEM+ANM	FDM	NEM+FDM

Table II. Comparison of NEM/FDM hybrid and VENTURE for the IAEA3D problem ($\Delta x = \Delta y = 10\text{cm}$)

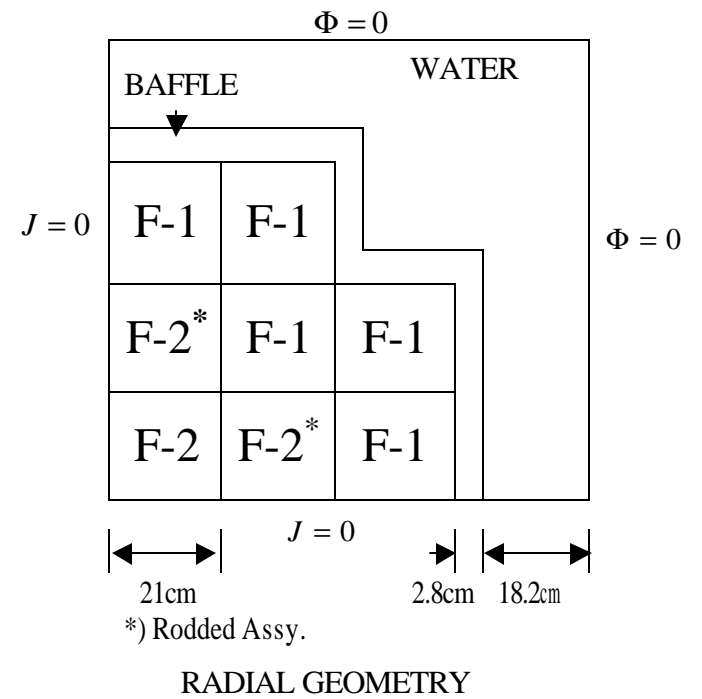
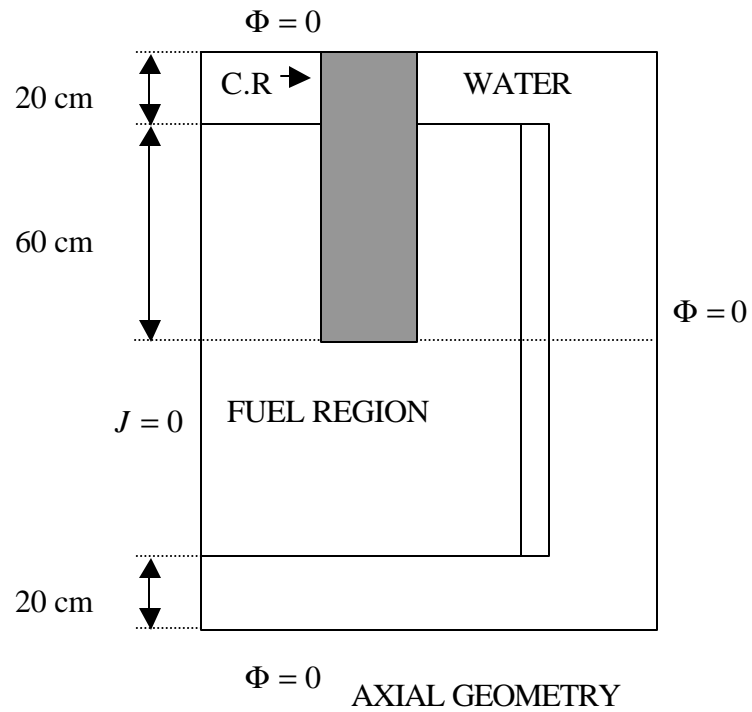
METHOD		k-eff	Computing Time(sec)
NEM/FDM HYBRID	$\Delta z = 5\text{ cm}$	1.029123	626
	$\Delta z = 10\text{ cm}$	1.029120	168
	$\Delta z = 20\text{ cm}$	1.029103	50
	$\Delta z = 30\text{ cm}$	1.029102	36
VENTURE	$\Delta z = 1\text{ cm}$	1.029122	1575
	$\Delta z = 2\text{ cm}$	1.029115	330
	$\Delta z = 4\text{ cm}$	1.029096	228
	$\Delta z = 10\text{ cm}$	1.029026	109
	$\Delta z = 0^*)$	1.029124	-

*) Extrapolated

Table III. Comparison of Hybrid Method and VENTURE for the Modified EPRI9R problem ($\Delta x = \Delta y = 1.4\text{cm}$)

METHOD		k-eff	Computing* Time(sec)
HYBRID	A	$\Delta z = 5\text{ cm}$	0.876659
		$\Delta z = 10\text{ cm}$	0.876729
		$\Delta z = 20\text{ cm}$	0.877018
	B	$\Delta z = 20\text{ cm}$	0.876896
	C	$\Delta z = 20\text{ cm}$	0.876782
VENTURE	$\Delta z = 1\text{ cm}$	0.876640	8079
	$\Delta z = 2\text{ cm}$	0.876639	2473
	$\Delta z = 5\text{ cm}$	0.876760	661
	$\Delta z = 10\text{ cm}$	0.877910	296
	$\Delta z = 20\text{ cm}$	0.882214	140

*) HP9000/777



ASSEMBLY
STRUCTURE

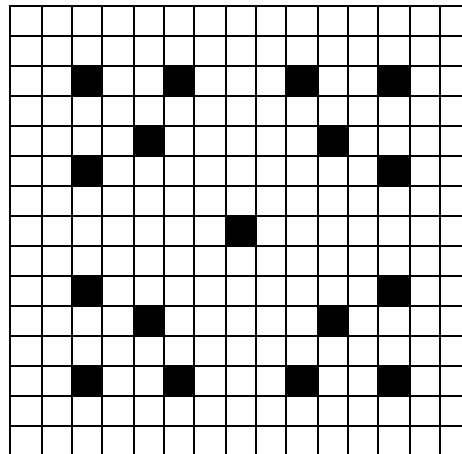


Figure 1. Modified 3-D EPRI-9R Benchmark Problem

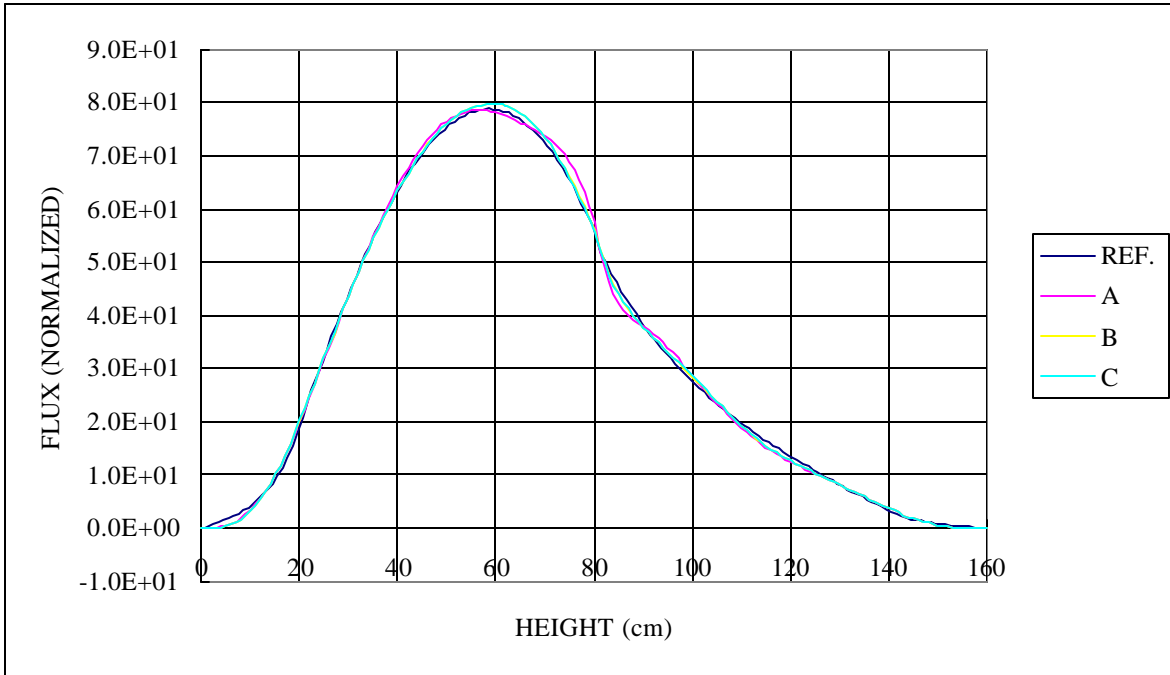


Figure 2. Fast Group Flux of a Rodded Cell

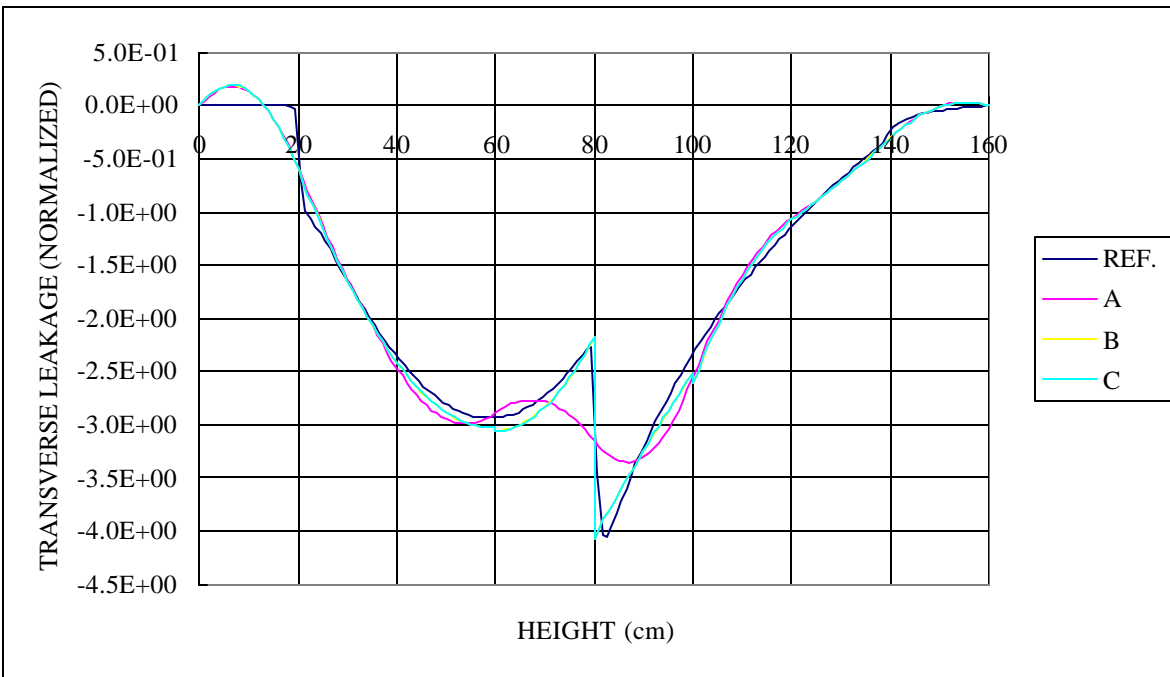


Figure 3. Fast Group Transverse Leakage of a Rodded Cell

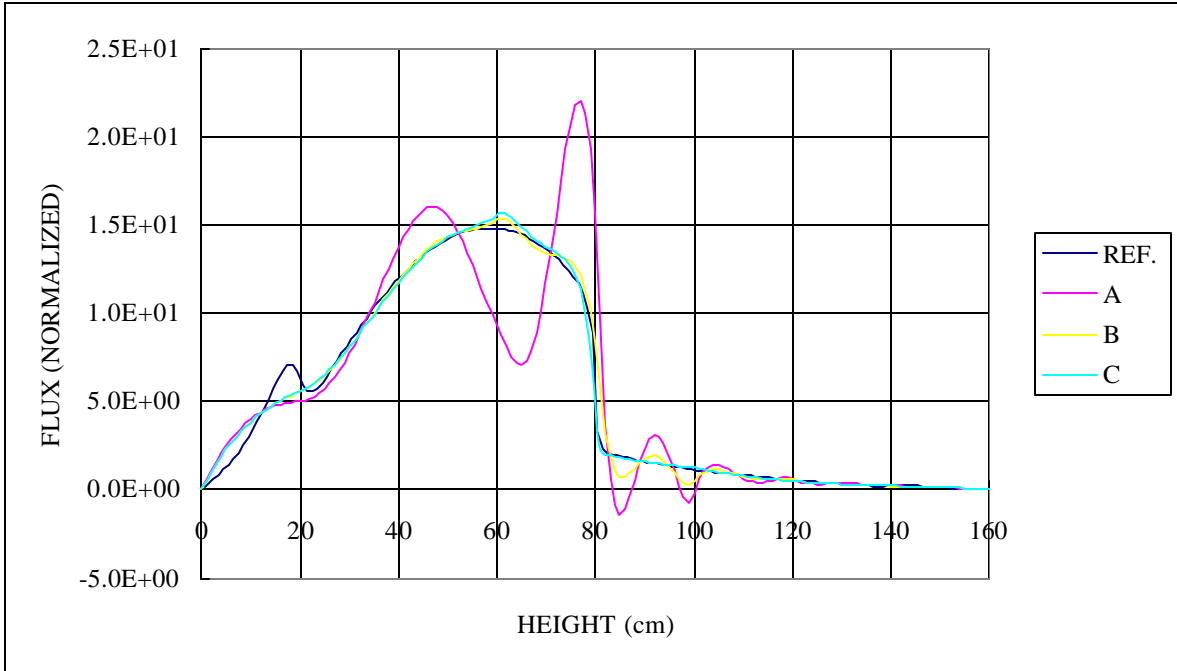


Figure 4. Thermal Group Flux of a Rodded Cell

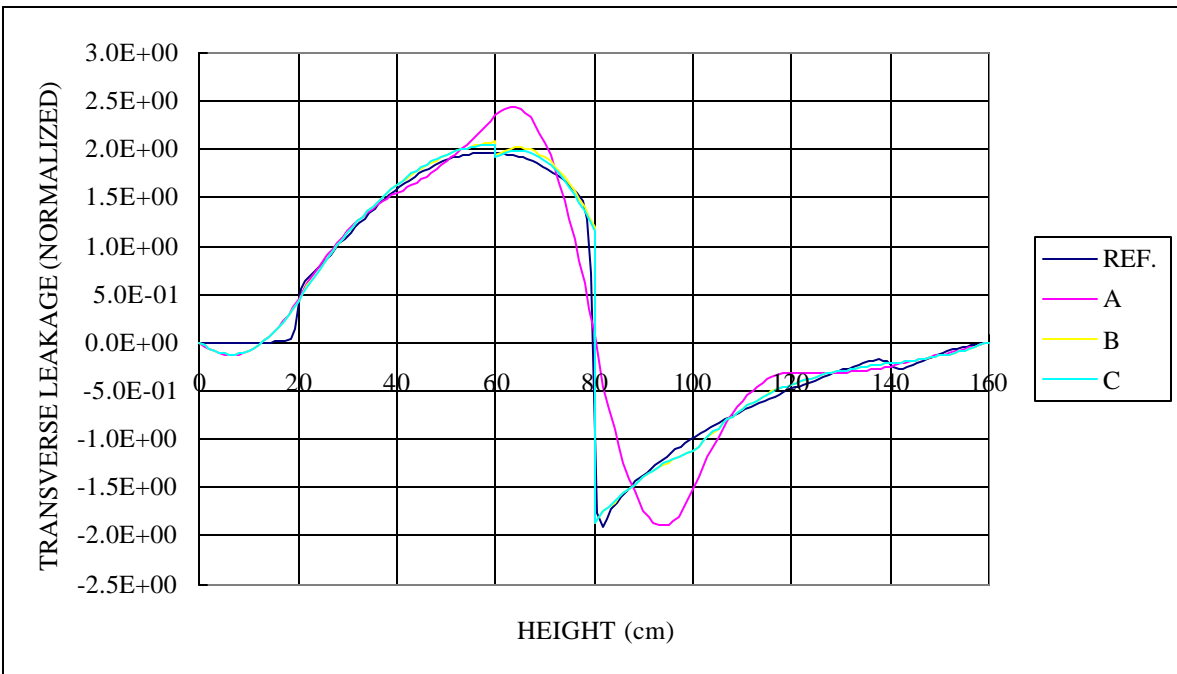


Figure 5. Thermal Group Transverse Leakage of a Rodded Cell

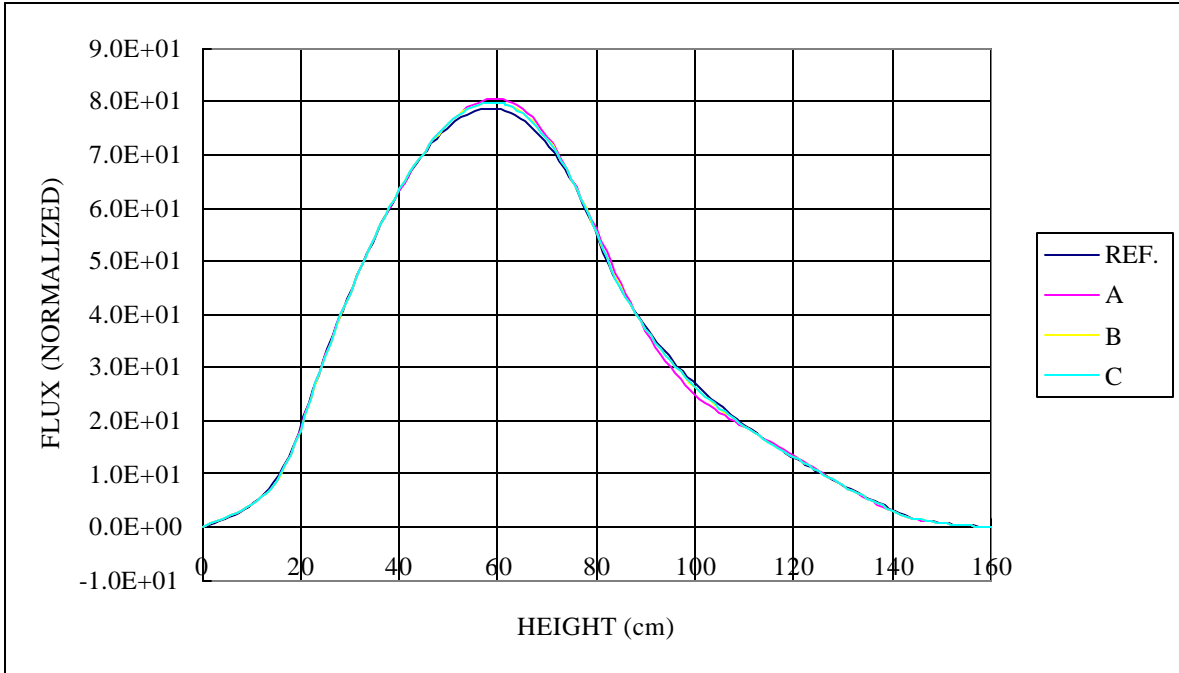


Figure 6. Fast Group Flux of a Fuel Cell

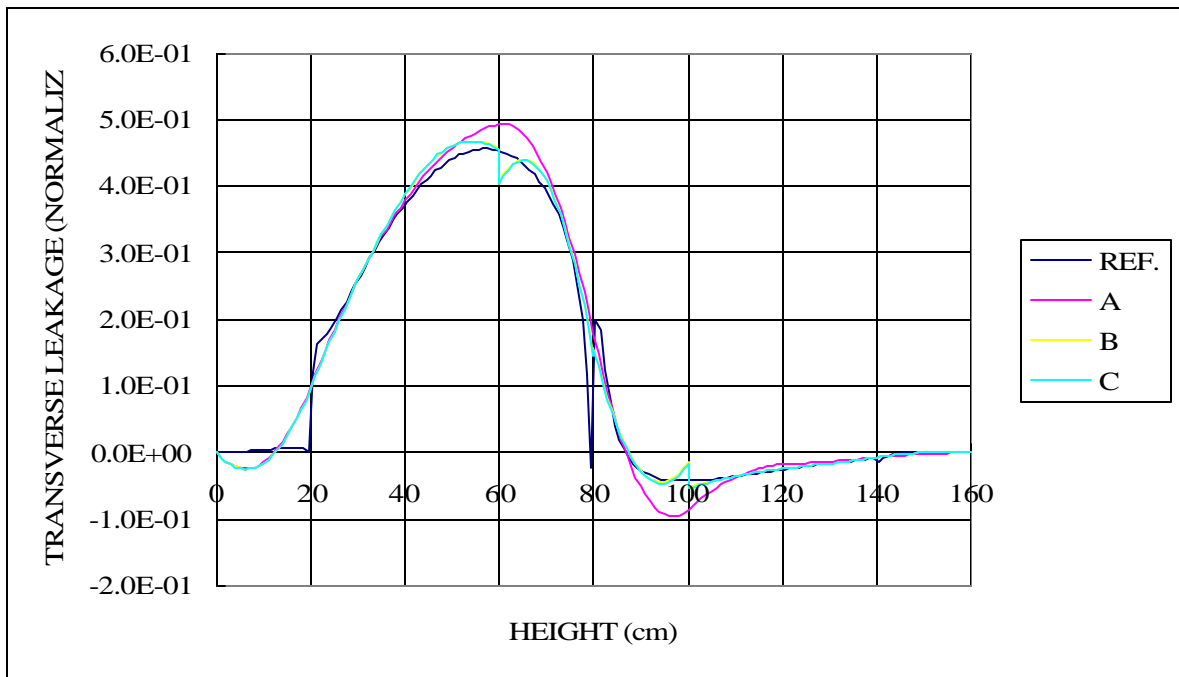


Figure 7. Fast Group Transverse Leakage of a Fuel Cell

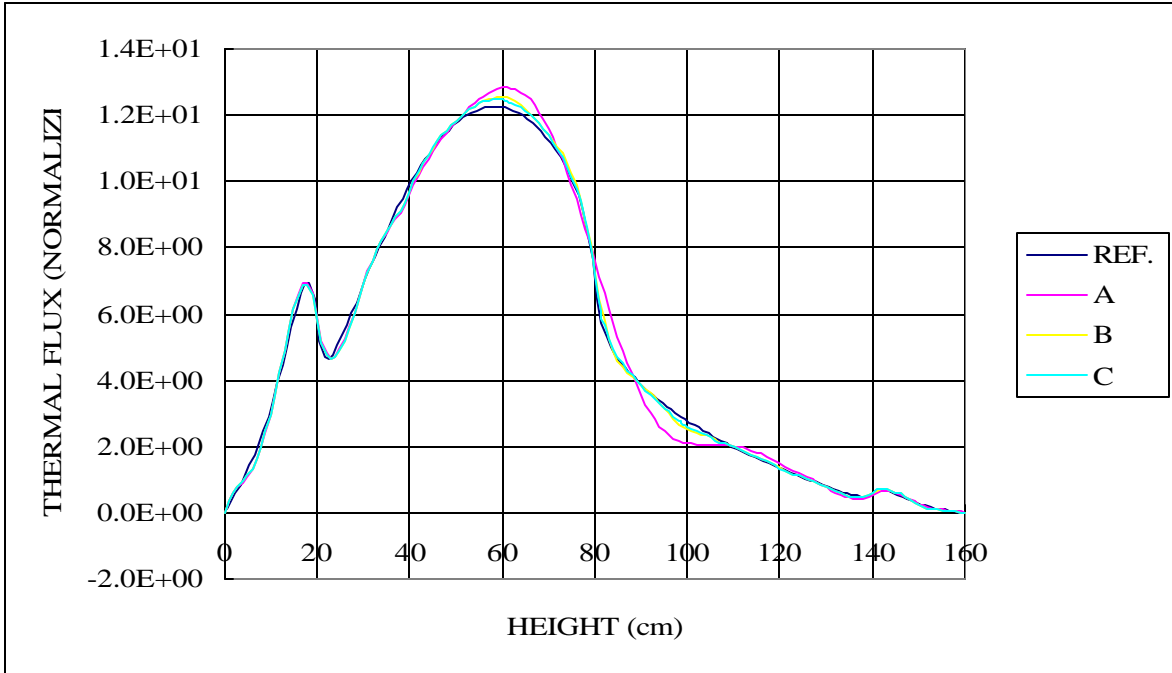


Figure 8. Thermal Group Flux of a Fuel Cell

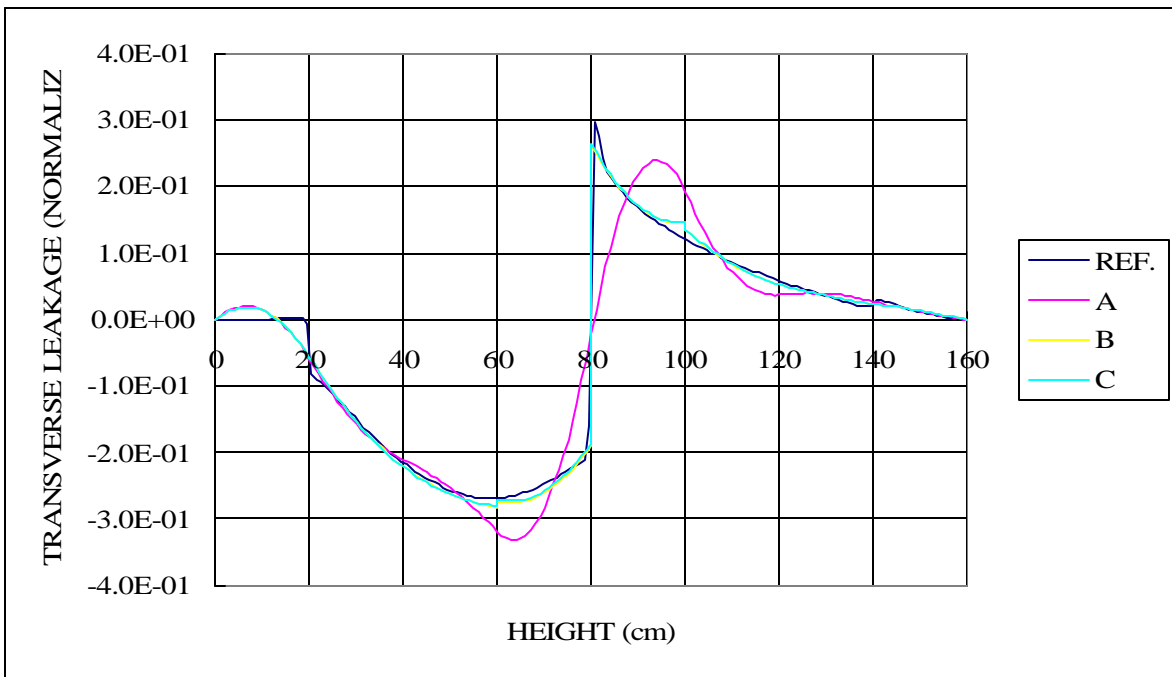


Figure 9. Thermal Group Transverse Leakage of a Fuel Cell

0.8860	0.6772	REF.	
0.8853	0.6759	A	
0.8855	0.6763	B	
0.8857	0.6766	C	
1.1007	1.2457	0.6772	
1.1031	1.2448	0.6759	
1.1025	1.2450	0.6763	
1.1019	1.2452	0.6766	
1.4263	1.1007	0.8860	Keff
1.4266	1.1031	0.8853	0.876640
1.4265	1.1025	0.8855	0.877018
1.4265	1.1019	0.8857	0.876896
			0.876782

Figure 10. Normalized Radial Power Distribution of Modified EPRI-9R Benchmark

1.3921	1.0417	REF.
1.4083	1.0498	A
1.4045	1.0483	B
1.4036	1.0482	C
1.8736	1.9659	1.0417
1.9128	1.9899	1.0498
1.9000	1.9842	1.0483
1.8935	1.9827	1.0482
2.2597	1.8736	1.3921
2.2891	1.9128	1.4083
2.2813	1.9000	1.4045
2.2793	1.8935	1.4036

Figure 11. Normalized Power Distribution in #4 Plane of Modified EPRI-9R Benchmark

.9382	.7579	REF.
.9334	.7555	A
.9357	.7569	B
.9358	.7572	C
.9183	1.3046	.7579
.9052	1.2448	.7555
.9120	1.3005	.7569
.9136	1.3007	.7572

1.4800	.9183	.9382
1.4727	.9052	.9334
1.4770	.9120	.9357
1.4768	.9136	.9358

Figure 12. Normalized Power Distribution in #5 Plane of Modified EPRI-9R Benchmark